available at www.sciencedirect.com
journal homepage: www.europeanurology.com

European Association of Urology

Prostate Cancer

Nodal Oligorecurrent Prostate Cancer: Anatomic Pattern of Possible Treatment Failure in Relation to Elective Surgical and Radiotherapy Treatment Templates

Aurélie De Bruycker[a,*], *Elise De Bleser*[b], *Karel Decaestecker*[b], *Valérie Fonteyne*[a], *Nicolaas Lumen*[b], *Pieter De Visschere*[c], *Kathia De Man*[d], *Louke Delrue*[c], *Bieke Lambert*[e,f], *Piet Ost*[a,*]

[a] *Department of Radiation Oncology and Experimental Cancer Research, Ghent University, Ghent, Belgium;* [b] *Department of Urology, Ghent University Hospital, Ghent, Belgium;* [c] *Department of Radiology, Ghent University Hospital, Ghent, Belgium;* [d] *Department of Radiology and Nuclear Medicine, Ghent University Hospital, Ghent, Belgium;* [e] *Department of Nuclear Medicine, AZ Maria Middelares and AZ Jan Palfijn, Ghent, Belgium;* [f] *Radiology and Nuclear Medicine, Ghent University, Ghent, Belgium*

Article info

Article history:
Accepted October 19, 2018

Associate Editor:
Giacomo Novara

Keywords:
Prostatic neoplasms
Neoplasm metastasis
Oligometastasis
Neoplasm recurrence
Choline positron emission tomography/computed tomography

Abstract

Background: Patients with biochemical recurrence following primary prostate cancer (PCa) treatment often experience relapse in the lymph nodes (LNs). Both salvage LN dissection (sLND) and elective nodal radiotherapy (ENRT) are potential treatment options.
Objective: To describe anatomic patterns of nodal oligorecurrent PCa in relation to different surgical and radiotherapy templates.
Design, setting, and participants: Patients with biochemical recurrence following primary PCa treatment were eligible for ^{18}F-choline positron emission tomography/computed tomography (CT). Patients with five or fewer LN recurrences (N1/M1a) were eligible for the current retrospective analysis.
Outcome measurements and statistical analysis: All LN recurrences were mapped on a reference patient CT, as well as different surgical templates (limited to superextended) and an adapted version of the PIVOTAL ENRT template, blinded for the recurrences. Descriptive statistics were used to report recurrences in relation to the different templates and to compare LN coverage between templates.
Results and limitations: In total, 158 LN recurrences (N1: 88; M1a: 70) in 82 patients (median age: 67 yr ; prostate-specific antigen [PSA]: 3.1 ng/ml; PSA doubling time of 7.8 mo at the time of clinical recurrence) were mapped. In 49% of patients, recurrences were exclusively located in the true pelvis, followed by the common iliac LN (10%), retroperitoneal/inguinal LN (10%), or a combination (31%). There was up to 40% volume overlap between ENRT and the surgical templates. Theoretically, with ENRT more patients are fully covered ($p < 0.02$) and the total number of covered lesions is higher ($p < 0.001$) when compared to all types of sLND, except for superextended sLND, which is comparable to ENRT (patient-level: $p = 0.6$; lesion-level: $p = 0.09$). With 22% of all 158 lesions located outside all templates (N1: 7%; M1a: 15%), at least 31% of all 82 patients would not be salvaged using any of the templates.
Conclusions: More than half of nodal recurrences are located outside the true pelvis. Limited or standard extended sLND is considered insufficient as a salvage treatment approach and is thus not recommended for use. To maximize treatment outcomes for nodal recurrences, ENRT or superextended sLND should be preferred.
Patient summary: We compared two possible treatment options, elective nodal radiotherapy and salvage lymph node dissection, for patients with prostate cancer recurrence limited to five or fewer lymph nodes and reported the nodal distrubution. Radiotherapy and surgery cover different areas with possible different outcomes.

* Corresponding authors. Department of Radiotherapy, Ghent University Hospital, Corneel Heymanslaan 10, B-9000 Ghent, Belgium. Tel. +32 3322411.
E-mail addresses: aurelie.debruycker@ugent.be (A. De Bruycker), piet.ost@ugent.be (P. Ost).

https://doi.org/10.1016/j.eururo.2018.10.044
0302-2838/

1. Introduction

Up to 30% of patients with high-risk prostate cancer (PCa) experience relapse after primary treatment [1]. Restaging with modern positron emission tomography (PET) tracers has indicated that the majority of patients experience relapse in the lymph nodes (LNs) [2–5]. For patients with limited or oligorecurrent nodes, local ablative therapies are being investigated, including stereotactic body radiotherapy (SBRT), elective nodal radiotherapy (ENRT), and salvage LN dissection (sLND) [6]. At present, it is unclear whether early identification and eradication of low-volume nodal recurrences changes the disease course for these patients. Only two phase 2 trials have been reported, with promising results for this patient population [7,8]. No phase 3 trials comparing different treatment approaches have been reported. A pure lesion-based approach (eg, SBRT) often misses PET-negative microscopic disease in neighbouring nodal areas, resulting in a need to repeat the treatment [7,8]. Both ENRT and sLND are being explored to treat both visible and microscopic oligorecurrent nodes. For both modalities, different templates have been suggested, but no data are available comparing the potential impact on outcomes.

The aim of the current study was to describe anatomic patterns of nodal oligorecurrent PCa in relation to different surgical and radiotherapy templates. Theoretically, this approach would allow us to estimate the number of lesions and patients that could be salvaged using these treatment approaches.

2. Patients and methods

2.1. Pattern of failures analysis

The primary outcome was anatomic mapping of LN recurrence following primary treatment and determination of the virtual coverage of these recurrences by salvage treatment options (ENRT and sLND). In addition, the coverage of ENRT and sLND templates was compared.

2.2. Patient selection

The local ethics committee (EC2012/308) approved this retrospective study. From 2011 to 2015, 229 patients underwent ^{18}F-choline PET/computed tomography (CT) for asymptomatic biochemical recurrence following primary PCa treatment (radical prostatectomy [RP] and/or radiotherapy [RT]) in accordance with the European Association of Urology (EAU) guidelines [1]; patients had a WHO performance score of 0–1 and testosterone of >50 ng/ml and were not on active treatment with any products known to influence prostate-specific antigen (PSA) [2]. Only patients with five or fewer LN recurrences on PET/CT were included in this retrospective analysis, since the benefit of sLND/ENRT is questionable if more than five lesions are present [9]. Patients who had received previous ENRT were excluded from the current analysis. Eighty-two men met these inclusion criteria (Supplementary Fig. 1). Details on confirmation of the PET-detected nodes are provided in the Supplementary material.

2.3. PET/CT LN mapping

^{18}F-Choline PET/CT imaging was performed 45 min after intravenous injection of 3–4 MBq of 18F-methylcholine as previously described [2]. PET/CT images were classified as positive or negative according to the presence of identified lesions by the nuclear medicine physician (B.L.) and radiologist (L.D.) [2]. The lesions detected on ^{18}F-choline PET/CT scans for all patients were transferred onto one uniform CT scan as spheres with a 2.5-mm radius. Using Mimics and 3-matic software (Materialise, Leuven, Belgium), the major blood vessels, ureters, prostate, rectum, and bladder were automatically delineated. Blinded to the lesions, an adapted version of the PIVOTAL LN template [10], including the common iliac LNs up to the aortic bifurcation (top of L4) [14], was manually drawn on the same CT image, as well as four different surgical templates: limited, standard, new extended, and superextended [11–13]. The software provided a tool to generate three-dimensional views of delineated contours. Subsequently, both still images and videos were created to visualize nodal oligorecurrences in relation to ENRT and sLND templates. A detailed description of all the templates and the delineation guide for ENRT can be found in the Supplementary material.

2.4. Statistical analysis

Quantitative analysis of the templates was conducted via Boolean operations using 3-matic software. Intersections between templates were expressed using the Jaccard overlap index (JI), calculated as follows:

$$\mathrm{JI} = \frac{\mathrm{V(intersection\ between\ ENRT\ and\ sLND\ templates)}}{\mathrm{V(union\ of\ ENRT\ and\ sLND\ templates)}}$$

Clinical and patient characteristics were reported using descriptive statistics. The McNemar test was used to compare patient and lesion coverage rates between different templates, with $p < 0.05$ considered significant (SPSS version 25; IBM, Armonk, NY, USA).

3. Results

3.1. Patient characteristics and LN distribution

In total, 158 LNs (N1: 88; M1a: 70) in 82 patients were mapped (Fig. 1). The clinical patient and tumour characteristics are listed in Table 1. The median age and PSA at diagnosis were 60 yr and 10.7 ng/ml, respectively, and 68.3% received multimodal treatment (RP + RT). At clinical recurrence, the median PSA and PSA doubling time (PSA-DT) were 3.1 ng/ml and 7.8 mo, respectively.

In 49% of patients, recurrences were exclusively located in the true pelvis, followed by the common iliac LNs (10%), retroperitoneal/distant inguinal LNs (10%), and a combination of these regions (31%). Both PSA and PSA-DT did not significantly differ between these groups. Of patients with pelvic LN recurrences only, the external iliac LNs were exclusively involved in 43% of the cases, followed by 30% of patients with internal iliac/obturator LN and 18% perirectal/presacral/paravesical LN lesions. In 11% of patients recurrences were observed in a combination of regions (Fig. 1).

3.2. Comparison of treatment templates and LN coverage

3.2.1. Visual comparison

Figure 2 shows a visual representation of all the templates. Videos depicting the different templates in relation to the lesions are available online. ENRT has a higher superior border compared to sLND templates and extends deeper into the presacral region (lower border of S2 and S3 for superextended sLND and ENRT, respectively). The surgical templates extend more distally along the external iliac

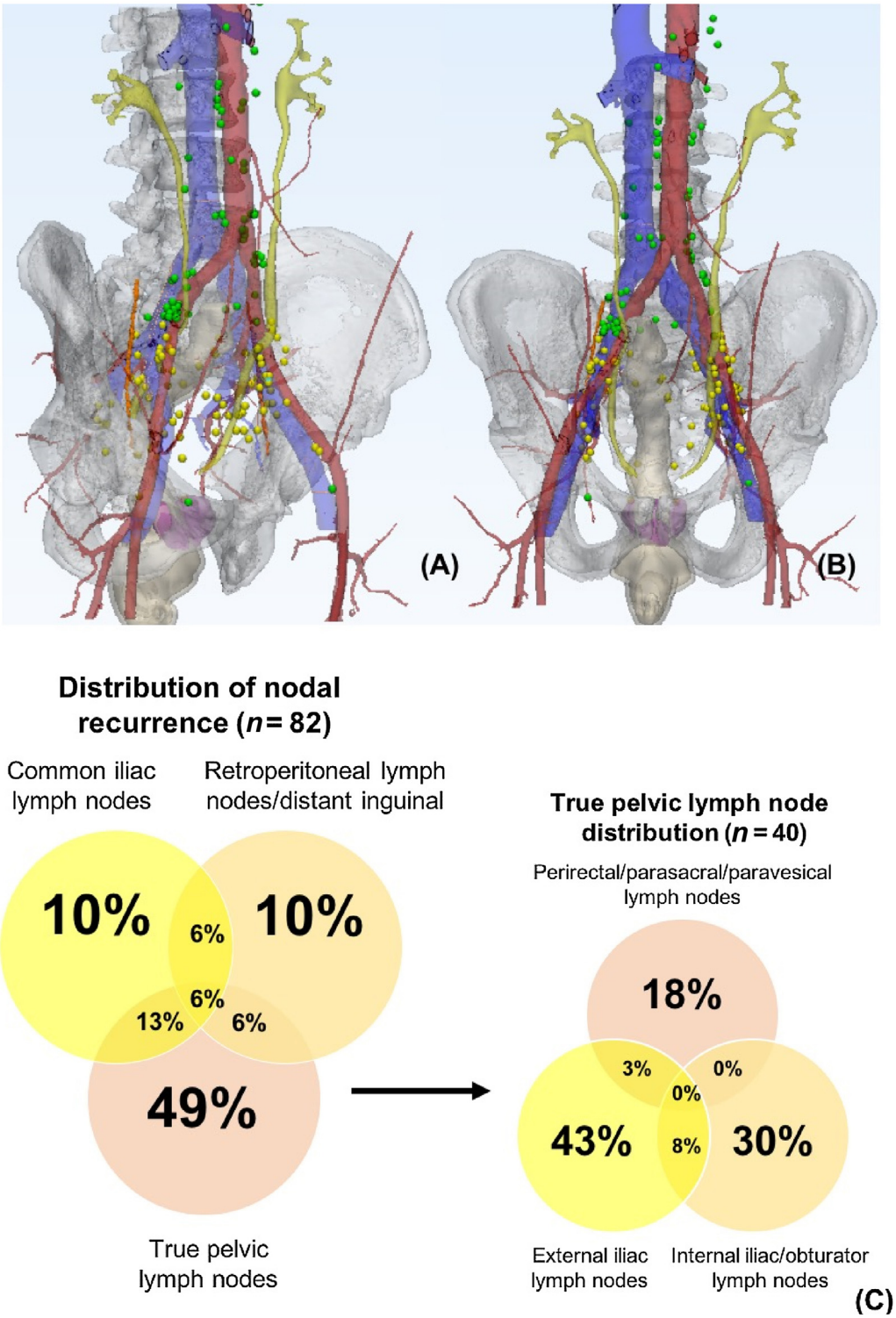

Fig. 1 – Three-dimensional virtual representation of 158 nodal recurrences in 82 patients (N1 lesions, yellow; M1a lesions, green) in (A) 45° profile and (B) frontal view. (C) Detailed Venn diagram displaying nodal relapse per lymph node (LN) station in relation to the true pelvis. Only two patients experienced an inguinal LN relapse. Arterial and venous structures are displayed in red and blue, and the urinary tract, prostate, and rectum in yellow, purple, and grey, respectively.

vessels as compared to ENRT. Lesions that are missed by all templates are located in the perirectal, presacral (below S3), retroperitoneal (especially above the aorta bifurcation), and inguinal regions.

3.2.2. Quantitative comparison

The volume of the different templates is shown in Supplementary Table 1, with ENRT and superextended sLND templates having the largest volume of 0.31 l. JI values,

Table 1 – Clinical patient and tumour characteristics for oligorecurrent prostate cancer after primary curative treatment

Characteristic	Pelvic recurrence	Extrapelvic recurrence	*p* value[a]
Patients (*n*)	40	42	
Median age at diagnosis, yr (IQR)	62 (57–68)	58 (53–62)	0.01
Median pretreatment PSA, ng/ml (IQR)	10.6 (7.8–14.3)	12 (7–19.2)	0.7
Gleason score, *n* (%)			0.07
≤6	9 (23)	11 (26)	
7	13 (33)	22 (52)	
8–10	18 (45)	9 (21)	
Tumour stage, *n* (%)			0.4
c/pT1	2 (5)	2 (5)	
c/pT2	19 (48)	17 (41)	
c/pT3	12 (30)	21 (50)	
c/pT4	3 (8)	1 (2)	
Missing	4 (10)	1 (2)	
N stage, *n* (%)			0.6
c/pN0	19 (48)	21 (50)	
c/pN1	0 (0)	1 (2)	
c/pNx	21 (53)	20 (48)	
Type of primary treatment, *n* (%)			0.2
Radical prostatectomy	3 (8)	9 (21)	
Radiotherapy ± ADT	7 (18)	5 (12)	
Combination	29 (73)	27 (64)	
Missing	1 (3)	1 (2)	
LN dissection at primary treatment, *n* (%)	19 (48)	25 (60)	0.5
Median LNs removed, *n* (IQR)	8 (4–13)	11 (7–14)	0.3
Median time from diagnosis to BCR, mo (IQR)	39.5 (24.8–65.5)	48.5 (27–90.8)	0.4
Median time from Dx to PET/CT$^+$, mo (IQR)	62 (44–103)	69 (46–112)	0.6
Median age at PET/CT$^+$, yr (IQR)	69 (63.3–71.8)	65 (58–71.3)	0.1
Median PSA at PET/CT$^+$, ng/ml (IQR)	2.8 (1.1–6.2)	3.3 (1.4–6.4)	0.6
Median PSA-DT at PET/CT$^+$, ng/ml (IQR)	9.3 (4.2–13.7)	6.6 (3.9–12.8)	0.4
Number of lesions at PET/CT$^+$, *n* (%)			0.002
1	20 (50)	7 (17)	
2	14 (35)	14 (33)	
3–5	6 (15)	21 (50)	

ADT = androgen deprivation therapy; LN = lymph node; BCR = biochemical recurrence; Dx = diagnosis; IQR = interquartile range; PET/CT = positive choline positron emission tomography/computed tomography imaging; PSA = prostate-specific antigen; PSA-DT = PSA doubling time.

[a] Comparison of characteristics between pelvic (N1 only) and extrapelvic recurrence (M1a only or N1 + M1a) using nonparametric tests (Mann–Whitney *U* test and χ^2). N1 lesions are defined as pelvic nodes below the bifurcation of the common iliac arteries and M1a lesions as distant metastases involving nonregional lymph nodes [1].

expressing the intersection rate between ENRT and sLND templates, ranged from 15% (limited) to 40% (superextended; Supplementary Table 1).

The number of patients and N1/M1a lesions theoretically covered by the different templates are depicted visually in Figure 2 and summarized in Tables 2 and 3. McNemar test results for comparison of coverage rates between the different templates are presented in Supplementary Tables 2 and 3.

With 22% of the lesions located outside all the templates (N1: 7%; M1a: 15%), at least 31% of the 82 patients would not be salvaged by any of the templates (Supplementary Tables 2 and 3; Fig. 3).

3.2.2.1. Detailed analysis of sLND templates. Both new and superextended sLND covered more N1 lesions compared to the limited and standard templates, but still missed 19% of N1 lesions (Table 3; Supplementary Tables 2 and 3). Limited and standard templates did not cover any M1a lesions. The superextended template covered more lesions than the new extended template ($p < 0.001$), but it still missed 49% of M1a lesions (Table 3; Supplementary Tables 2 and 3). All perirectal and approximately all retroperitoneal nodes were missed by sLND.

3.2.2.2. Detailed analysis of ENRT templates. ENRT missed 20% of N1 lesions (Table 3; Supplementary Table 2). Full coverage of the obturator, presacral, and internal iliac nodes was obtained, but all perirectal nodes were missed, in addition to 26% of external iliac nodes (Table 3; Supplementary video). The updated PIVOTAL covered 29% more M1a lesions than the RTOG/PIVOTAL templates.

3.2.2.3. Comparison between sLND and ENRT templates. The number of patients ($p = 0.6$) and lesions ($p = 0.09$) covered was comparable between ENRT and superextended sLND, at 62% and 59%, respectively (Table 2), which was significantly more patients compared to any other surgical template ($p \leq 0.02$; Supplementary Tables 2 and 3). ENRT covered 22–49% more patients and 20–56% more lesions compared to sLND (limited to the new extended template; $p \leq 0.02$; Supplementary Tables 2 and 3).

The coverage rate for N1 lesions was comparable between ENRT and the new and superextended sLND templates, and was significantly higher compared to the limited and standard extended sLND templates ($p < 0.001$; Supplementary Tables 2 and 3). The detailed analysis of pelvic nodes described in Table 3 showed that perirectal

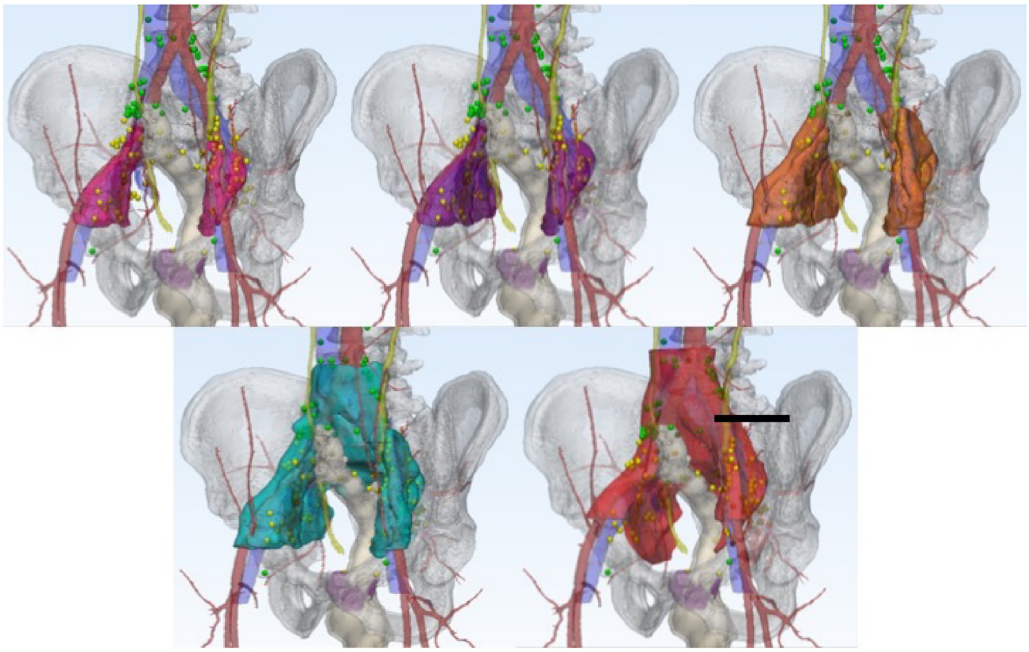

Fig. 2 – Virtual representation of all recurrences (N1, yellow; M1a, green) in relation to the different theoretical treatment templates. From left to right, the limited, standard extended, and new extended salvage lymph node dissection (sLND) templates on the upper line and the super extended sLND and radiotherapy templates on the lower line are shown. The black line indicates the L5/S1 interspace, depicting the height of delineation using the RTOG/PIVOTAL templates for elective nodal radiotherapy.

Table 2 – Patient coverage for the different sLND templates compared to ENRT

	Patient coverage, *n* (%)				
	sLND template				ENRT
	Limited	Standard	New extended	Superextended	
Within the template	13 (16)	22 (27)	39 (48)	48 (59)	51 (62)
Outside the template	69 (84)	60 (73)	43 (52)	34 (41)	31 (38)

ENRT = elective nodal radiotherapy; sLND = salvage lymph node dissection.

Table 3 – Lesion coverage by salvage treatment per anatomic region

	Total no. of lesions per region (*n* = 158)	Lesions covered by template, *n* (%)				
		ENRT (*n* =115)	sLND template			
			Limited (*n* = 32)	Standard (*n* = 49)	NE (*n* = 91)	SE (*n* = 107)
Remaining retroperitoneal LN	21	0 (0)	0 (0)	0 (0)	0 (0)	0 (0)
Upper border L4-ABF	9	9 (100)	0 (0)	0 (0)	1 (11)	1 (11)
Common iliac LN (ABF-L5/S1)	38 [a]	36 (95)	0 (0)	0 (0)	19 (50)	35 (92)
True pelvis (below L5/S1)	88	70 (80)	32 (36)	49 (56)	71 (81)	71 (81)
External iliac LN	45	38 (84)	28 (62)	31 (69)	44 (98)	43 (96)
Internal iliac LN	15	14 (93)	1 (7)	4 (27)	12 (80)	11 (73)
Obturator LN	15	15 (100)	2 (13)	13 (87)	14 (93)	14 (93)
Presacral LN	2	2 (100)	0 (0)	0 (0)	0 (0)	2 (100)
Perirectal LN	10	0 (0)	0 (0)	0 (0)	0 (0)	0 (0)
Paravesical LN	1	1 (100)	1 (100)	1 (100)	1 (100)	1 (100)
Inguinal LN (M1a)	2	0 (0)	0 (0)	0 (0)	0 (0)	0 (0)

ABF = aorta bifurcation; ENRT = elective nodal radiotherapy, NE = new extended; LN = lymph node; SE = superextended; sLND = salvage lymph node dissection.
[a] One LN located in mesenteric tissue at the level of the common iliac vessels, not covered by any of the templates.

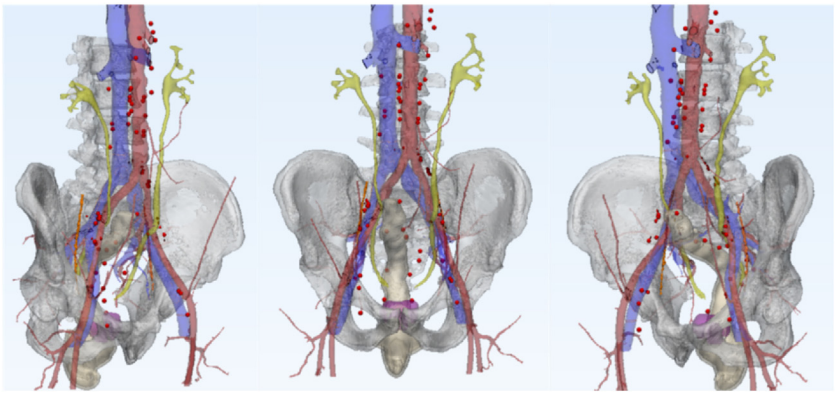

Fig. 3 – Profile and frontal views of the nodal recurrences (red spheres) missed by both elective nodal radiotherapy and salvage lymph node dissection templates.

nodes were missed by all the treatment options, while presacral nodes were fully covered by ENRT and superextended sLND. ENRT missed 12% more external iliac nodes compared to superextended sLND, which in turn missed ±14% more internal iliac/obturator nodes compared to ENRT.

ENRT covered more M1a lesions than new and superextended sLND ($p \leq 0.002$; Supplementary Tables 2 and 3). To obtain approximately full coverage (92–95%; Table 3) of the common iliac nodes, in which 10% of the patients experienced relapse solely (Fig. 2), ENRT or superextended sLND needs to be performed. By contrast, limited or standard sLND covered no common iliac nodes and new extended sLND only covered up to 50%. One-third of retroperitoneal nodes were covered by ENRT, compared to only 3% for superextended sLND (Table 3).

4. Discussion

Recent data suggest that LNs provide a gateway to hematogenous metastases [15,16] and nodal recurrences are the most dominant relapse pattern following maximal local therapy [2–5]. Consequently, elective or salvage nodal treatments might delay progression or improve survival for patients with limited LN metastases, as has been suggested by retrospective and limited prospective data [7–9,17]. However, sufficient coverage of micrometastatic disease is required to observe a benefit of nodal treatments. We mapped 158 nodal recurrences identified in 82 patients on a reference patient to estimate the potential impact of different salvage treatments.

The pattern of failure observed in this study shows that limiting the treatment field to the true pelvis would cover only half of the recurrences. Moreover, it is clear that sLND and ENRT templates do not cover all pelvic recurrences. Both limited and standard sLND are insufficient, with coverage of only 36% and 56%, respectively, of pelvic lesions. The new extended, superextended, and ENRT templates are comparable, with coverage of 80–81% of pelvic lesions, but still missing approximately one in five lesions. To improve coverage, ENRT templates should extend more distally along the external iliac fields, as done in the sLND templates (Supplementary videos). This extension would increase the lesion coverage at this level from 84% (distal limit: top of the femoral head) to 98% (distal limit: midfemoral head). ENRT, by contrast, provides greater coverage along the internal iliac field. More aberrant locations (eg, perirectal nodes, accounting for 11% of pelvic lesions) are not covered by any of the templates.

Approximately 26% of recurrences are observed exclusively outside the true pelvis, and 25% in both the pelvis and extrapelvic areas, mostly at the level of the common iliac or retroperitoneal LNs (Fig. 1). This has also been observed by others using conventional CT [13], choline PET/CT [18], prostate-specific membrane antigen (PSMA) PET/CT [5,19], and surgical series [20]. Spratt et al. [13] reported that ±55% of patients experienced relapse in the common iliac region. Joniau et al. [20] also noted that 21% of pelvic recurrences were in the common iliac nodes. Thus, we can conclude that the common iliac nodal site is an important region of recurrence and should be taken into account when salvage therapy is performed. To ensure complete coverage of this region, the upper border for ENRT should be based on the patient's individual anatomy. If a standardized bony anatomy surrogate is chosen, we would recommend L4 as the upper border, which would increase lesion coverage from 44% (limit at L5/S1) to 73% (limit at the top of L4). These results are comparable to the study by Parker et al. [18], who found that 43% and 67% of all lesions were covered for delineation up to the level of L5/S1 and L4/L5, respectively. For sLND, a superextended template ensures coverage of 92% of the common iliac nodes, compared to only 50% for new extended sLND.

Even with ENRT up to the top border of L4, 38% of all patients would not be salvaged, with 27% of all lesions missed. These numbers closely resemble the 3-yr progression-free survival (PFS) rate of 62–75% after ENRT for nodal recurrences [21–24]. The same holds true for superextended sLND, which missed 41% of patients and 32% of lesions. In the majority of sLND series, smaller standard or extended templates are followed [25]. These sLND data were analysed in a recent systematic review by Brassetti

et al. [31], who concluded that sLND is not associated with a durable response over time, since 54–94% of patients experience biochemical recurrence within 5 yr. These results are comparable to the reported 3-yr and 5-yr PFS results after SBRT of 34% and 13%, respectively [21,26]. When looking at the pattern of recurrence following sLND, it is striking that 60% of patients develop new nodal recurrences, confirming the high rate of microscopic LNs missed [27]. The same recurrence pattern is observed with SBRT, with 68% of relapses following SBRT located in the nodes [21,26].

At present it is unclear whether early identification and eradication of low-volume nodal recurrences changes the disease course in this patient population, a concern also expressed by Murphy et al. [28]. Two prospective phase 2 trials reported promising results after metastasis-directed therapy for PET-detected recurrences, with excellent local control and low toxicity [7,8]. However, a large proportion of patients experience biochemical recurrence within 1 yr, followed by a new clinical recurrence. These results highlight the limitations of a true lesion-directed approach when relying on novel imaging. Our results support the possible benefit of more comprehensive approaches such as ENRT and superextended sLND [6,22,29]. Results from ongoing trials, such as OLIGOPELVIS (NCT02274779), will provide prospective data on PFS and ENRT toxicity as compared to intermittent androgen deprivation therapy (ADT). The randomised phase 2 STORM trial (NCT03569241) will randomise patients to SBRT/sLND ± ENRT in combination with temporary ADT. The primary endpoint is time to the development of metastatic disease. The results will improve our knowledge of the pattern of relapse and outcome for these different approaches. Alternatively, trials such as RTOG-0534 will inform us if nodal recurrences can be avoided by implementing ENRT at the time of salvage RT of the prostate bed. The first results are expected in October 2018.

We acknowledge certain limitations to our study. First, histological confirmation of nodal relapses was obtained in only 29% of our cohort; however, we tried to maximize confirmation of disease via the addition of sequential imaging and follow-up of PSA levels and PSA response following treatment, similar to other studies [3,30].

Second, as choline PET/CT is the standard imaging modality recommended for restaging in the EAU guidelines, other tracers (eg, ^{68}Ga PSMA) were not assessed. We acknowledge the higher accuracy for detection of clinical recurrence of PSMA-targeted imaging and its capability of visualizing lesions earlier in the disease course at lower PSA values [4,5]. However, it appears from a PSMA-based study by Calais et al. [5] that the location of nodal recurrences is comparable to our findings. They reported that the RTOG template missed 24% of true pelvic nodes, compared to 20% in our study. The authors did not mention surgical templates or alternative radiotherapy templates such as PIVOTAL. Consequently, we believe that our results remain valid in the PSMA era.

Although this was a retrospective analysis, all the ^{18}F-choline PET/CT scans were interpreted by the same experts in nuclear medicine (B.L.) and radiology (L.D.) to preserve consistency. All the lesions were mapped manually, blinded from the templates to avoid bias.

Finally, our study was designed to obtain data for comparison of elective or salvage treatment options, but it does not attempt to validate a certain clinical benefit of sLND or ENRT. However, Abdollah et al. [9] reported retrospective data suggesting that these nodal treatment options might delay progression or improve survival at a limited nodal disease burden, which makes our comparison valuable.

5. Conclusions

More than half of nodal recurrences are located outside the true pelvis. Limited or standard extended sLND is considered insufficient as a salvage treatment approach and is thus not recommended for use. To maximize treatment outcomes for nodal recurrences, ENRT or superextended sLND should be preferred.

Author contributions: Aurélie De Bruycker had full access to all the data in the study and takes responsibility for the integrity of the data and the accuracy of the data analysis.

Study concept and design: De Bruycker, Ost, Decaestecker.
Acquisition of data: De Bruycker, Ost, Decaestecker.
Analysis and interpretation of data: De Bruycker, Ost, Decaestecker.
Drafting of the manuscript: Piet Ost, Aurélie De Bruycker.
Critical revision of the manuscript for important intellectual content: Fonteyne, Lambert, Decaestecker, De Bleser, De Visschere, De Man, Lumen, Delrue.
Statistical analysis: De Bruycker, Ost, De Bleser.
Obtaining funding: None.
Administrative, technical, or material support: Ost, Decaestecker.
Supervision: Ost.
Other: None.
Financial disclosures: Aurélie De Bruycker certifies that all conflicts of interest, including specific financial interests and relationships and affiliations relevant to the subject matter or materials discussed in the manuscript (eg, employment/affiliation, grants or funding, consultancies, honoraria, stock ownership or options, expert testimony, royalties, or patents filed, received, or pending), are the following: None.
Funding/Support and role of the sponsor: None.

Appendix A. Supplementary data

Supplementary data associated with this article can be found, in the online version, at https://doi.org/10.1016/j.eururo.2018.10.044.

References

[1] Mottet N, can den Bergh RCN, Briers E, et al. EAU-ESTRO-ESUR-SIOG guidelines on prostate cancer. European Association of Urology; 2018. http://uroweb.org/guideline/prostate-cancer/.
[2] De Bruycker A, Lambert B, Claeys T, et al. Prevalence and prognosis of low-volume, oligorecurrent, hormone-sensitive prostate cancer amenable to lesion ablative therapy. BJU Int 2017;120:815–21.
[3] Parker WP, Davis BJ, Park SS, et al. Identification of site-specific recurrence following primary radiation therapy for prostate cancer using C-11 choline positron emission tomography/computed to-

mography: a nomogram for predicting extrapelvic disease. Eur Urol 2017;71:340–8.
[4] Perera M, Papa N, Christidis D, et al. Sensitivity, specificity, and predictors of positive ^{68}Ga-prostate-specific membrane antigen positron emission tomography in advanced prostate cancer: a systematic review and meta-analysis. Eur Urol 2016;70:926–37.
[5] Calais J, Czernin J, Cao M, et al. ^{68}Ga-PSMA-11 PET/CT mapping of prostate cancer biochemical recurrence after radical prostatectomy in 270 patients with a PSA level of less than 1.0 ng/mL: impact on salvage radiotherapy planning. J Nucl Med 2018;59:230–7.
[6] De Bleser E, Tran PT, Ost P. Radiotherapy as metastasis-directed therapy for oligometastatic prostate cancer. Curr Opin Urol 2017;27:587–95.
[7] Ost P, Reynders D, Decaestecker K, et al. Surveillance or metastasis-directed therapy for oligometastatic prostate cancer recurrence: a prospective, randomized, multicenter phase II trial. J Clin Oncol 2018;36:446–53.
[8] Siva S, Bressel M, Murphy DG, et al. Stereotactic abative body radiotherapy (SABR) for oligometastatic prostate cancer: a prospective clinical trial. Eur Urol 2018;74:455–62.
[9] Abdollah F, Dalela D, Sood A, et al. Impact of adjuvant radiotherapy in node-positive prostate cancer patients: the importance of patient selection. Eur Urol 2018;74:253–6.
[10] Harris VA, Staffurth J, Naismith O, et al. Consensus guidelines and contouring atlas for pelvic node delineation in prostate and pelvic node intensity modulated radiation therapy. Int J Radiat Oncol Biol Phys 2015;92:874–83.
[11] Ploussard G, Briganti A, de la Taille A, et al. Pelvic lymph node dissection during robot-assisted radical prostatectomy: efficacy, limitations, and complications—a systematic review of the literature. Eur Urol 2014;65:7–16.
[12] Maderthaner L, Furrer MA, Studer UE, Burkhard FC, Thalmann GN, Nguyen DP. More extended lymph node dissection template at radical prostatectomy detects metastases in the common iliac region and in the fossa of Marcille. BJU Int 2018;121:725–31.
[13] Spratt DE, Vargas HA, Zumsteg ZS, et al. Patterns of lymph node failure after dose-escalated radiotherapy: implications for extended pelvic lymph node coverage. Eur Urol 2017;71:37–43.
[14] Shih HA, Harisinghani M, Zietman AL, Wolfgang JA, Saksena M, Weissleder R. Mapping of nodal disease in locally advanced prostate cancer: rethinking the clinical target volume for pelvic nodal irradiation based on vascular rather than bony anatomy. Int J Radiat Oncol Biol Phys 2005;63:1262–9.
[15] Brown M, Assen FP, Leithner A, et al. Lymph node blood vessels provide exit routes for metastatic tumor cell dissemination in mice. Science 2018;359:1408–11.
[16] Pereira ER, Kedrin D, Seano G, et al. Lymph node metastases can invade local blood vessels, exit the node, and colonize distant organs in mice. Science 2018;359:1403–7.
[17] Steuber T, Jilg C, Tennstedt P, et al. Standard of care versus metastases-directed therapy for PET-detected nodal oligorecurrent prostate cancer following multimodality treatment: a multi-institutional case-control study. Eur Urol Focus. In press. https://doi.org/10.1016/j.euf.2018.02.015.
[18] Parker WP, Evans JD, Stish BJ, et al. Patterns of recurrence after postprostatectomy fossa radiation therapy identified by C-11 choline positron emission tomography/computed tomography. Int J Radiat Oncol Biol Phys 2017;97:526–35.
[19] Schiller K, Sauter K, Dewes S, et al. Patterns of failure after radical prostatectomy in prostate cancer – implications for radiation therapy planning after 68Ga-PSMA-PET imaging. Eur J Nucl Med Mol Imaging 2017;44:1656–62.
[20] Joniau S, Van den Bergh L, Lerut E, et al. Mapping of pelvic lymph node metastases in prostate cancer. Eur Urol 2013;63:450–8.
[21] Fodor A, Lancia A, Ceci F, et al. Oligorecurrent prostate cancer limited to lymph nodes: getting our ducks in a row. World J Urol. In press. https://doi.org/10.1007/s00345-018-2322-7.
[22] Wurschmidt F, Petersen C, Wahl A, Dahle J, Kretschmer M. [^{18}F] Fluoroethylcholine-PET/CT imaging for radiation treatment planning of recurrent and primary prostate cancer with dose escalation to PET/CT-positive lymph nodes. Radiat Oncol 2011;6:44.
[23] Schick U, Jorcano S, Nouet P, et al. Androgen deprivation and high-dose radiotherapy for oligometastatic prostate cancer patients with less than five regional and/or distant metastases. Acta Oncol 2013;52:1622–8.
[24] Fodor A, Berardi G, Fiorino C, et al. Toxicity and efficacy of salvage carbon 11-choline positron emission tomography/computed tomography-guided radiation therapy in patients with lymph node recurrence of prostate cancer. BJU Int 2017;119:406–13.
[25] Herlemann A, Kretschmer A, Buchner A, et al. Salvage lymph node dissection after 68Ga-PSMA or 18F-FEC PET/CT for nodal recurrence in prostate cancer patients. Oncotarget 2017;8:84180–92.
[26] Ost P, Jereczek-Fossa BA, Van As N, et al. Pattern of progression after stereotactic body radiotherapy for oligometastatic prostate cancer nodal recurrences. Clin Oncol 2016;28:e115–20.
[27] Rischke HC, Schultze-Seemann W, Wieser G, et al. Adjuvant radiotherapy after salvage lymph node dissection because of nodal relapse of prostate cancer versus salvage lymph node dissection only. Strahlenther Onkol 2015;191:310–20.
[28] Murphy DG, Sweeney CJ, Tombal B. "Gotta catch 'em all", or do we? Pokemet approach to metastatic prostate cancer. Eur Urol 2017;72:1–3.
[29] Ponti E, Lancia A, Ost P, et al. Exploring all avenues for radiotherapy in oligorecurrent prostate cancer disease limited to lymph nodes: a systematic review of the role of stereotactic body radiotherapy. Eur Urol Focus 2017;3:538–44.
[30] Lecouvet FE, El Mouedden J, Collette L, et al. Can whole-body magnetic resonance imaging with diffusion-weighted imaging replace Tc 99m bone scanning and computed tomography for single-step detection of metastases in patients with high-risk prostate cancer? Eur Urol 2012;62:68–75.
[31] Brassetti A, et al. Oligometastatic prostate cancer and salvage lymph node dissection: systematic review. Minerva Chir 2018. http://dx.doi.org/10.23736/S0026-4733.18.07796-9, [Epub ahead of print].